Impact of dust aerosols on the retrieval of IR land surface emissivity spectrum:

A new simultaneous approach accounting for dust characteristics and surface temperature from IASI

V. Capelle, A. Chédin, C. Crevoisier, R. Armante, L. Cr epeau, and N. A. Scott

LMD / IPSL, Ecole Polytechnique, Palaiseau, France

Rationale

- Create a new IR surface emissivity database from IASI
- Higher spatial resolution than previous (0.5° => 0.25°)
- High spectral resolution (0.05µm from 3.7 to 14µm)
- Clean from dust contamination
- Day and night separate
- Global
- Monthly

First step: creation of a monthly climatology averaging the 10 years of IASI data

- Create a new IR surface emissivity database from IASI
- **Higher spatial resolution than previous (0.5° => 0.25°)**
- **High spectral resolution (0.05µm from 3.7 to 14µm)**
- **Clean from dust contamination**
- **Day and night separate**
- **Global**
- Monthly

Impact of surface parameters on BT spectrum

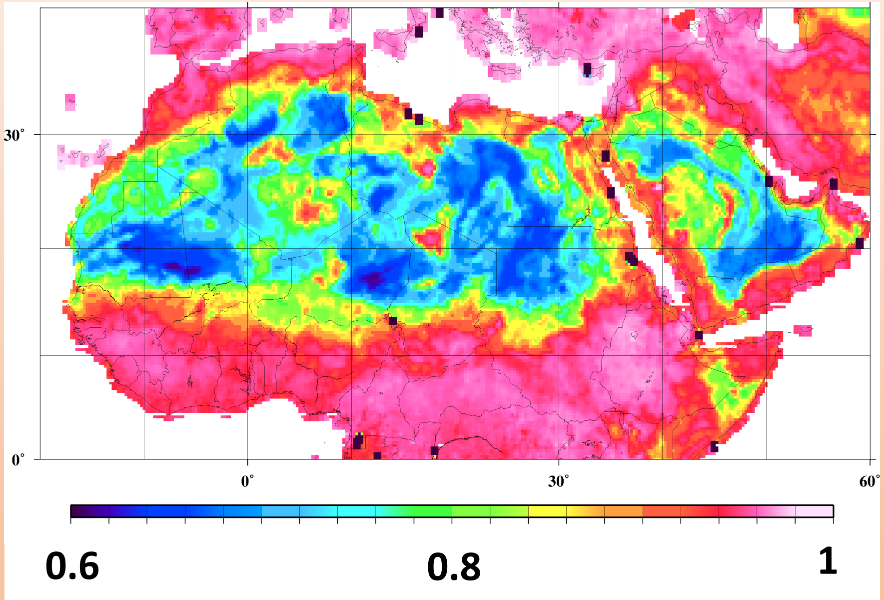

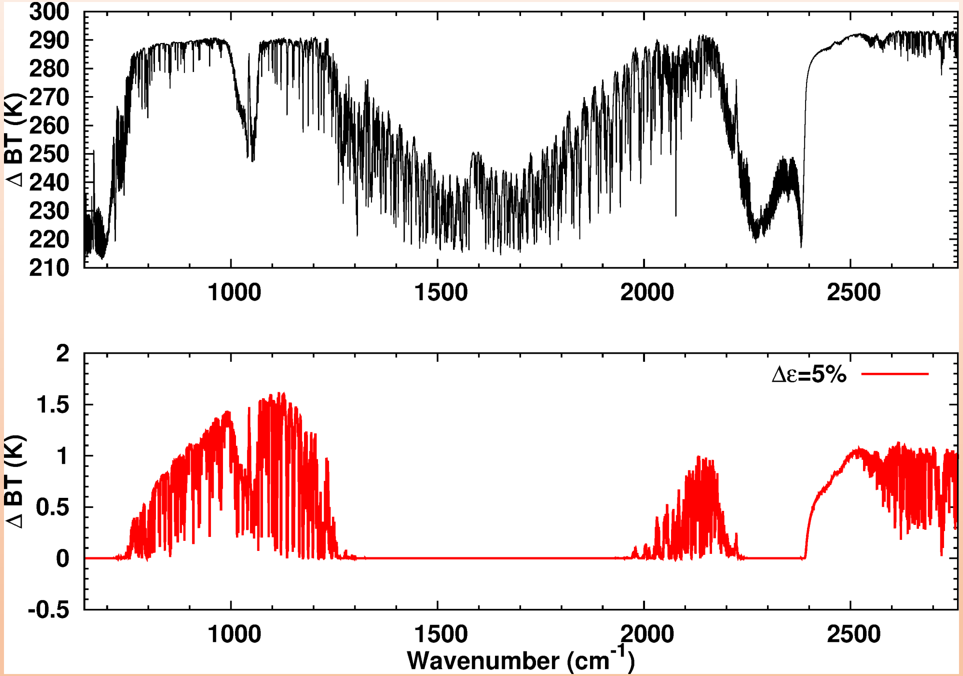

Variation of emissivity larger than 20% in few km

5% of emissivity (~ 0.05) => 1.5K in BT

Impact of surface parameters on BT spectrum

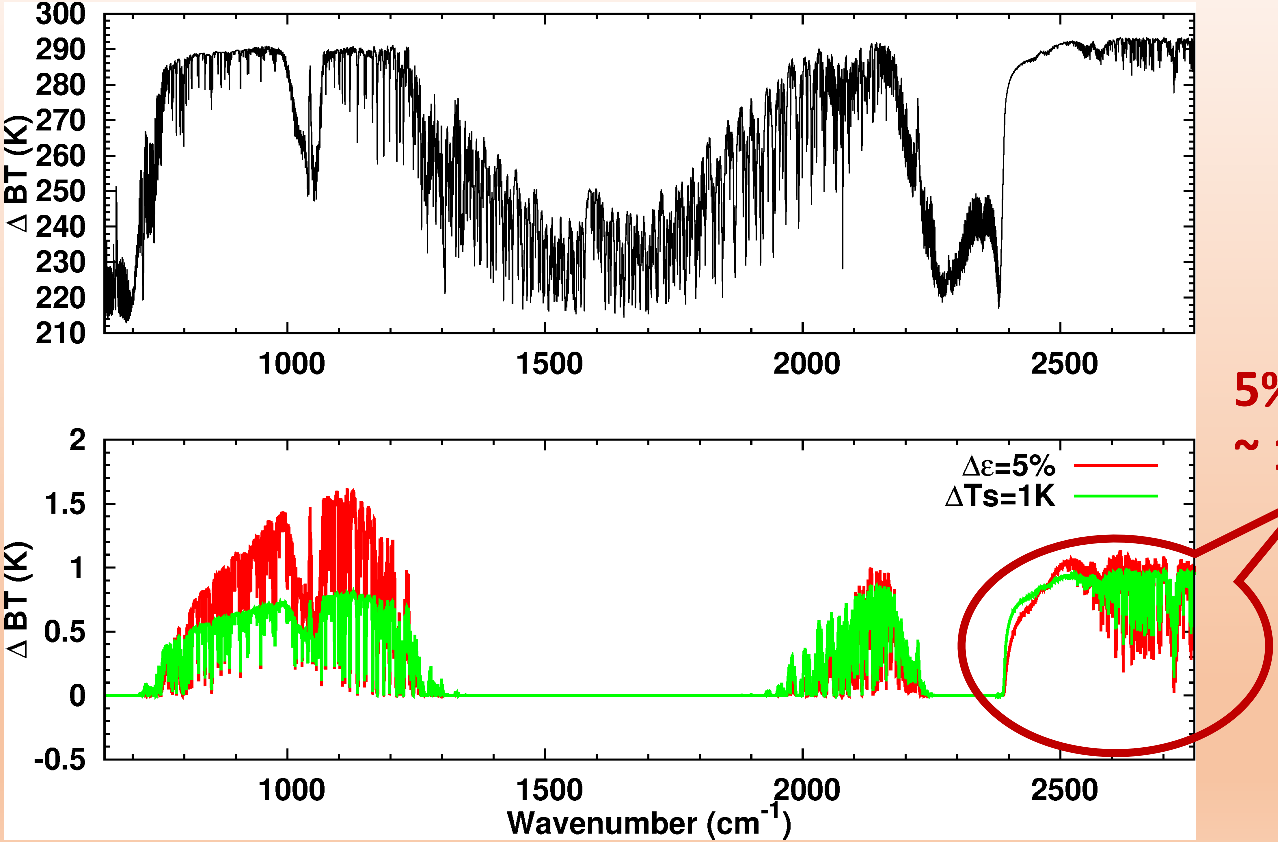

5% of emissivity
~ 1K of Tsurf

Impact of surface parameters on BT spectrum

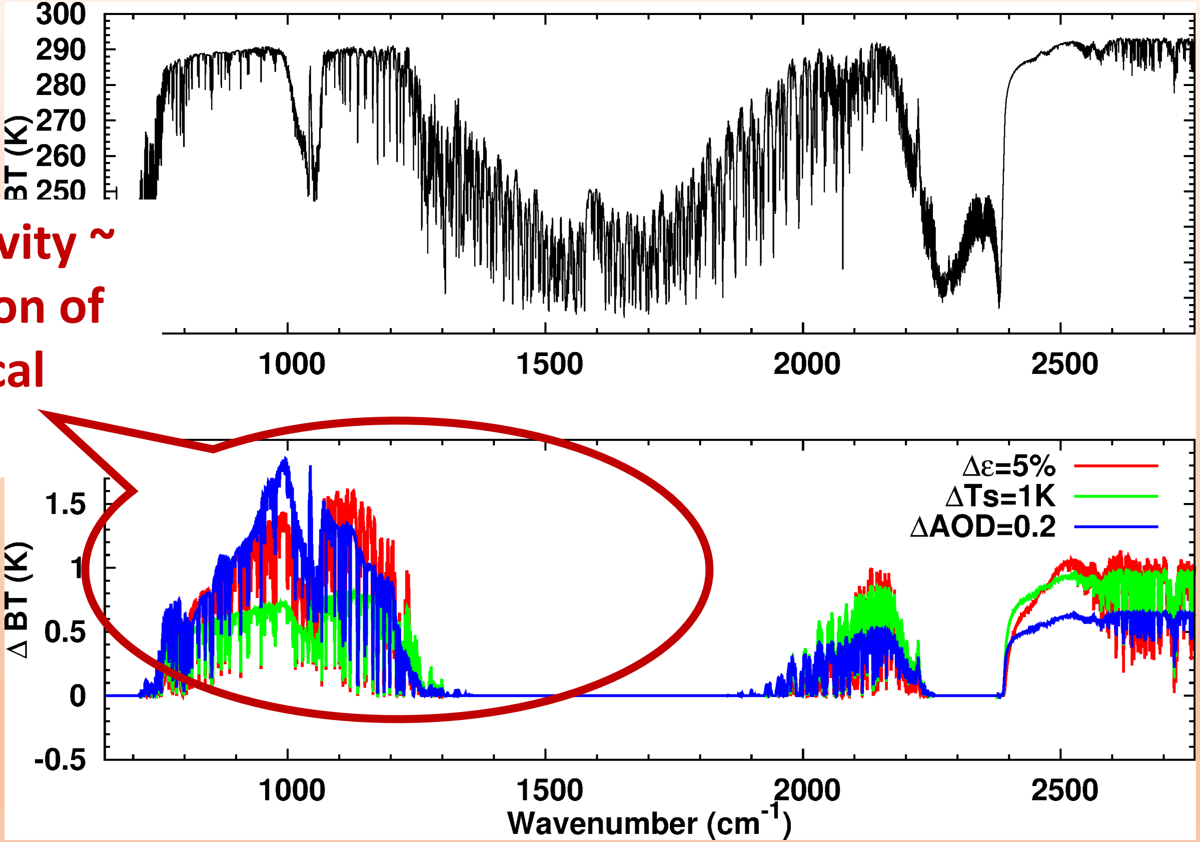

5% of emissivity ~ small variation of aerosol optical depth (AOD)

=> Estimating surface parameters requires precise knowledge of aerosol properties and/or a severe filtering.

Possibility of dust filtering?
Statistics on the 2007-2017 IASI period

January

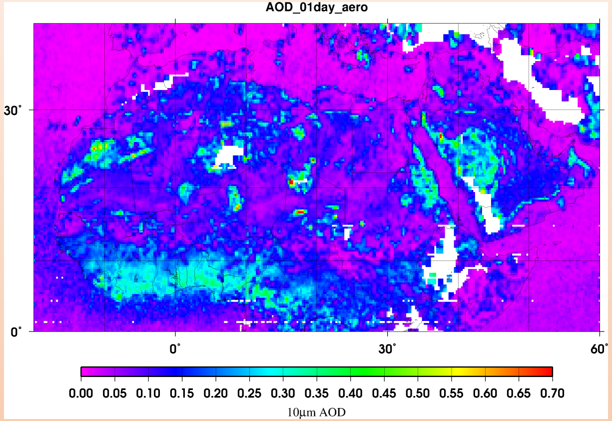

July

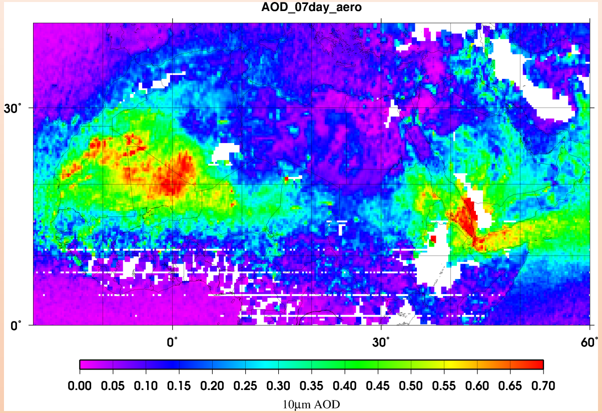

Mean of 10 μm Dust AOD

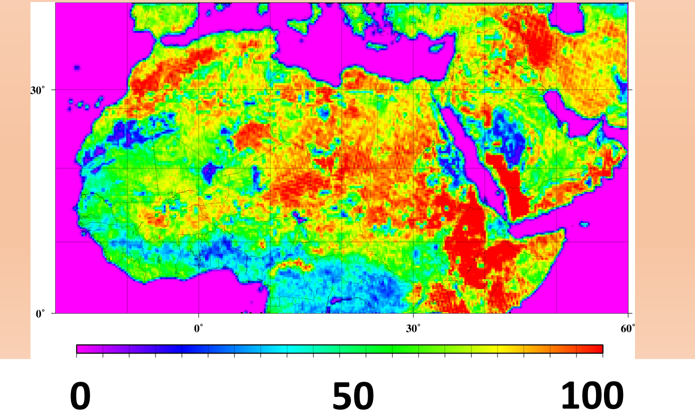

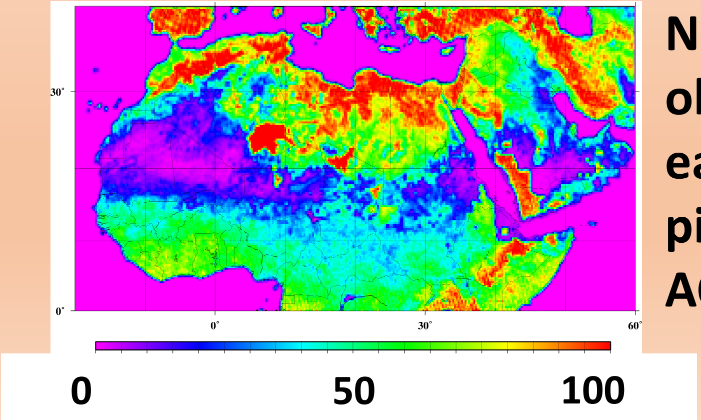

Number of observation in each 0.25° pixel grid with AOD<0.15

Possibility of dust filtering?
Statistics on the 2007-2017 IASI period

January | **July**

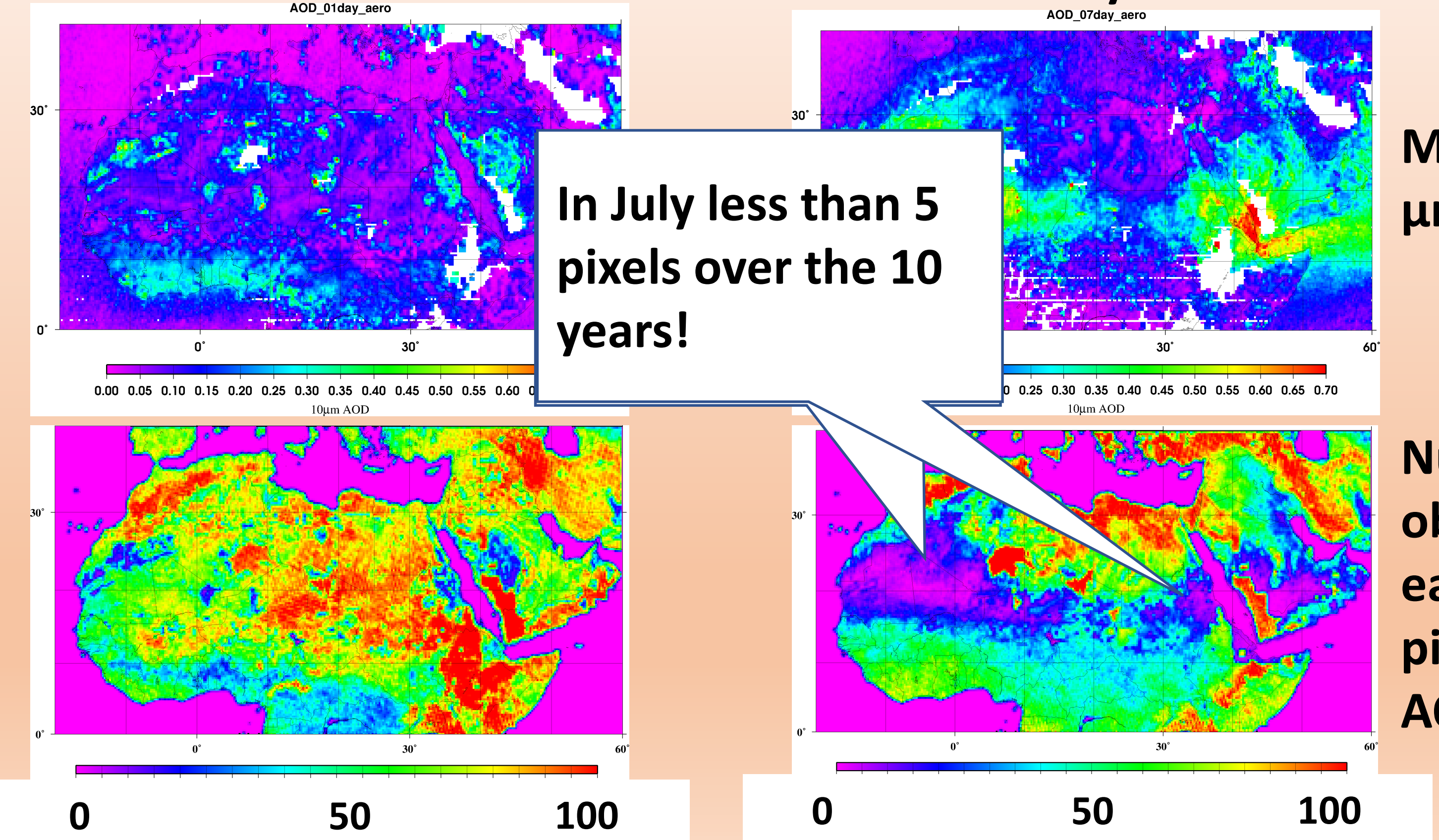

Mean of 10 µm Dust AOD

Number of observation in each 0.25° pixel grid with AOD<0.15

Expected seasonal variation of emissivity: NDVI seasonal variation as proxy

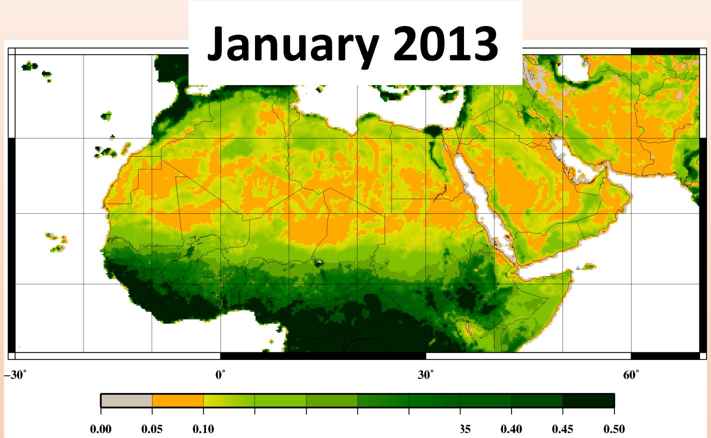

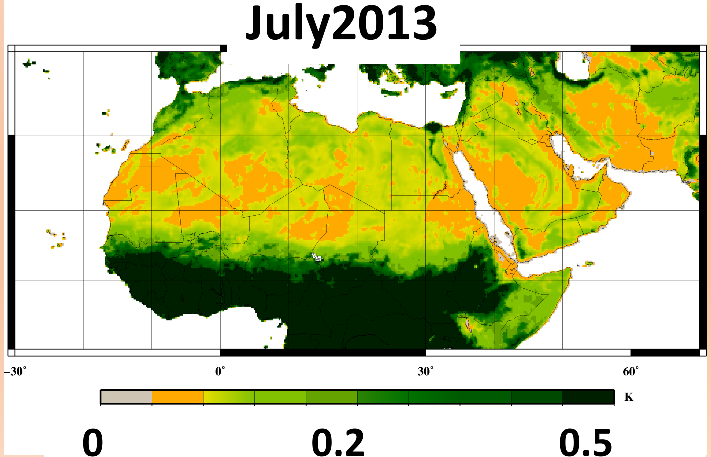

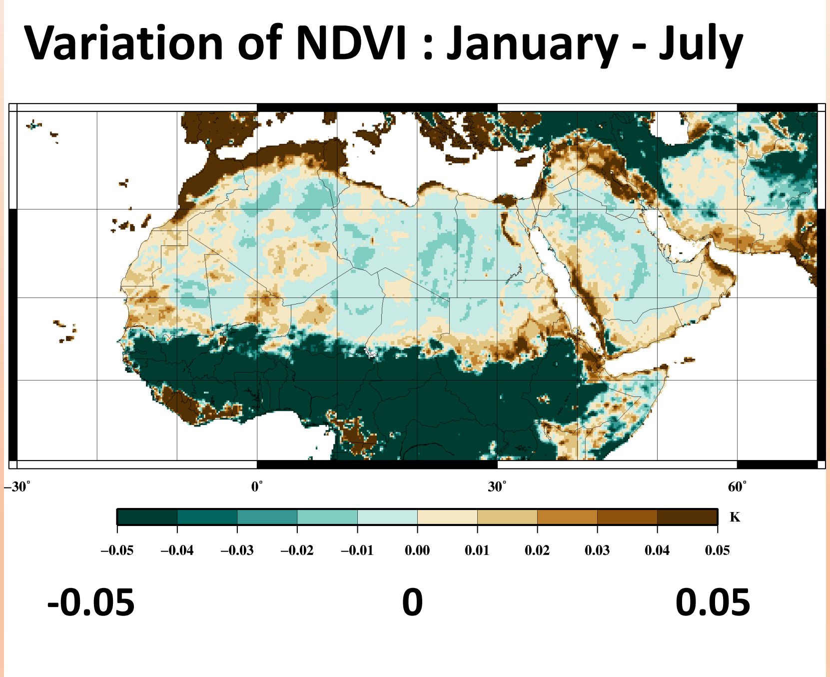

Impact of dust on Emissivity databases

Surface emissivity at 8.3µm (January 2013)

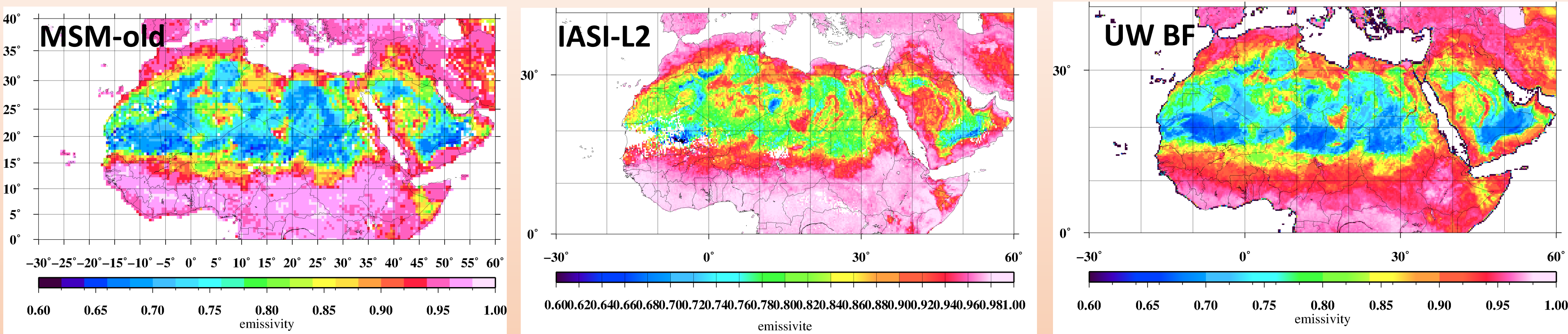

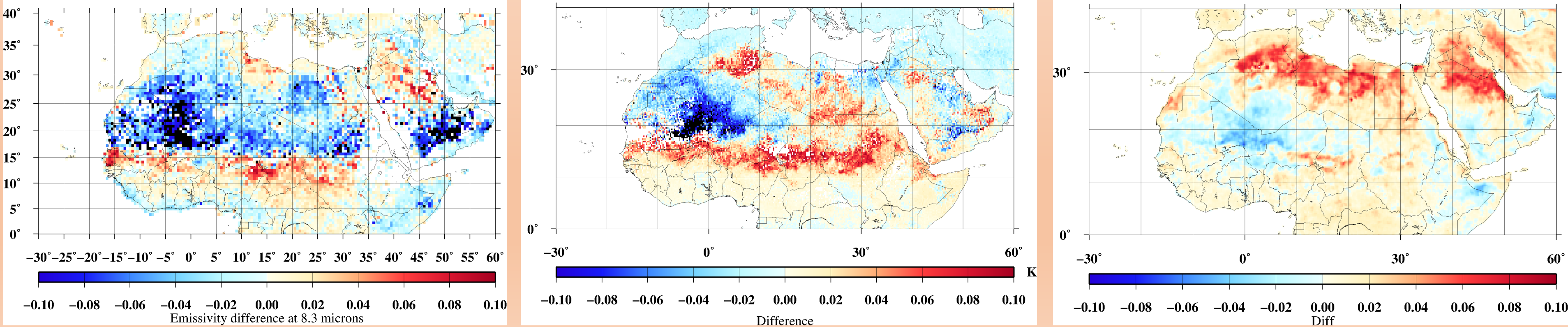

Surface emissivity difference at 8.3µm (January –July 2013)

Impact of dust on Emissivity databases

Surface emissivity at 3.7µm (January 2013)

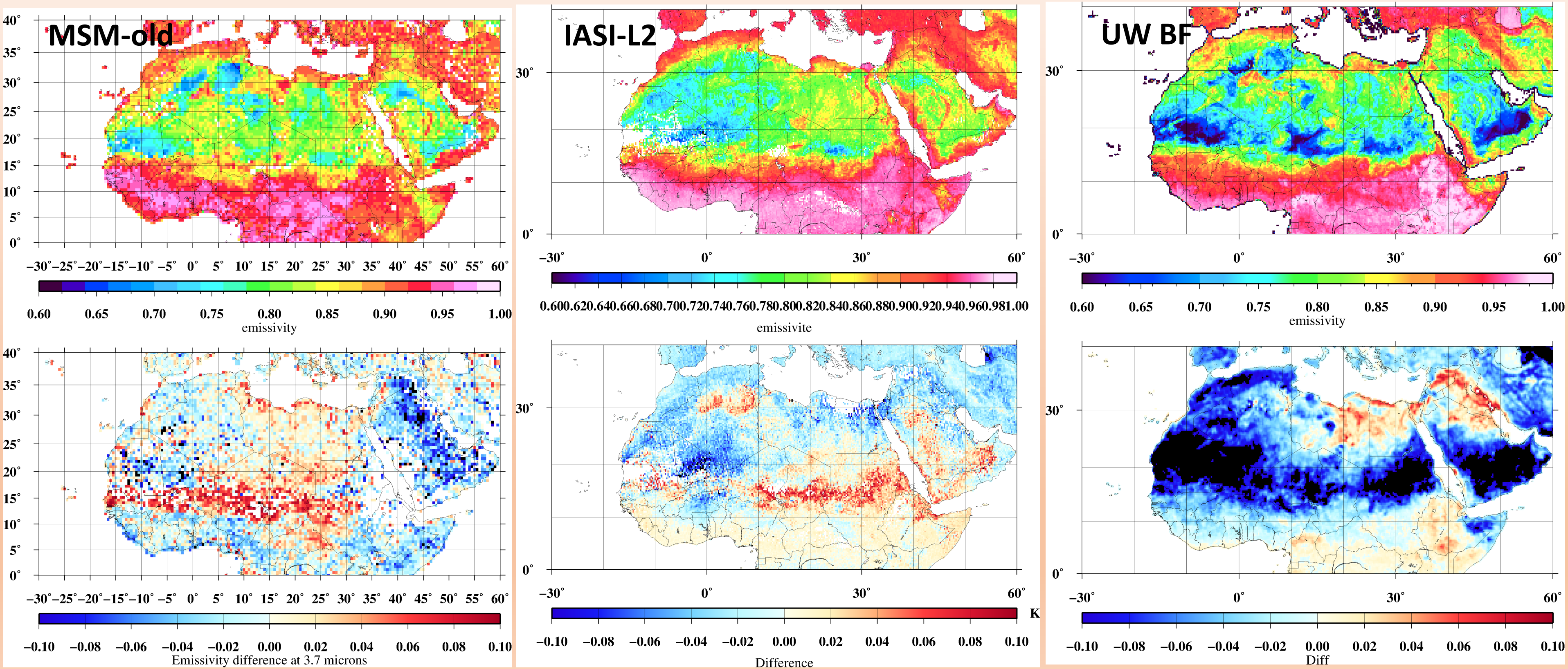

Surface emissivity difference at 3.7µm (January –July 2013)

Joint surface/aerosol inversion scheme : an iterative process

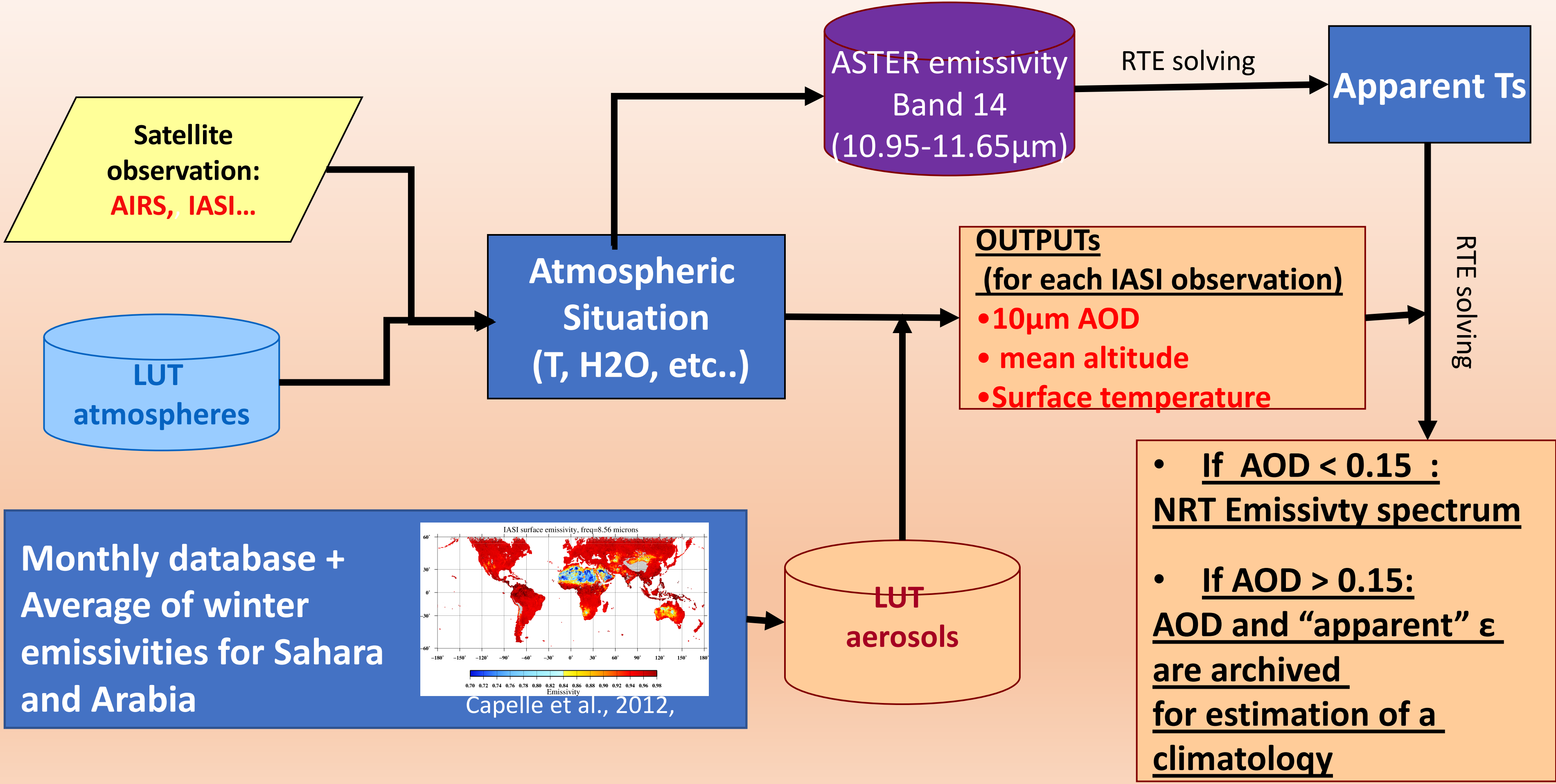

Dust + emissivity coupling: AOD/emissivity correlation

AOD/emissivity at 8.3µm correlation: July 2007-2017; daytime

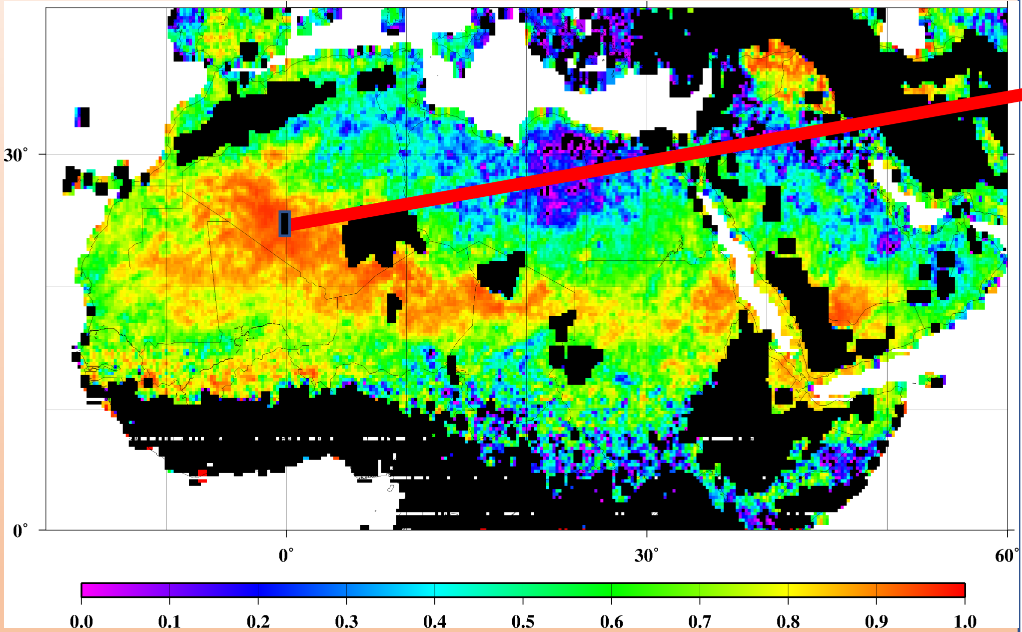

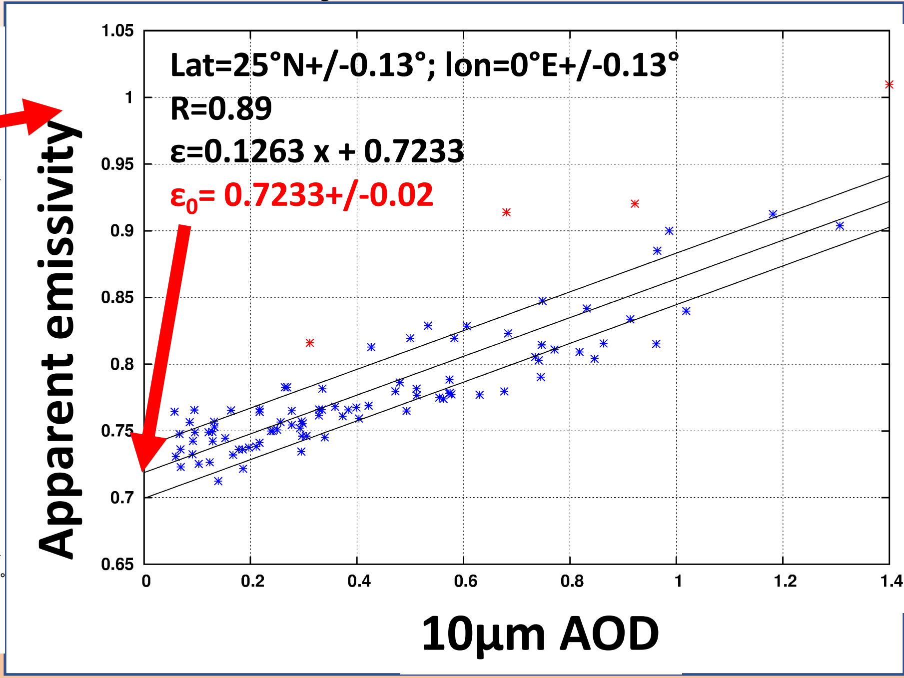

- ⇒ **AOD/emissivity correlation computed for each pixel of a 0.25° grid and for a selection of window channels**
- ⇒ **ε obtained by regression**

Dust + emissivity coupling: AOD/emissivity correlation

AOD/emissivity at 4.63µm correlation: July 2007-2017; daytime

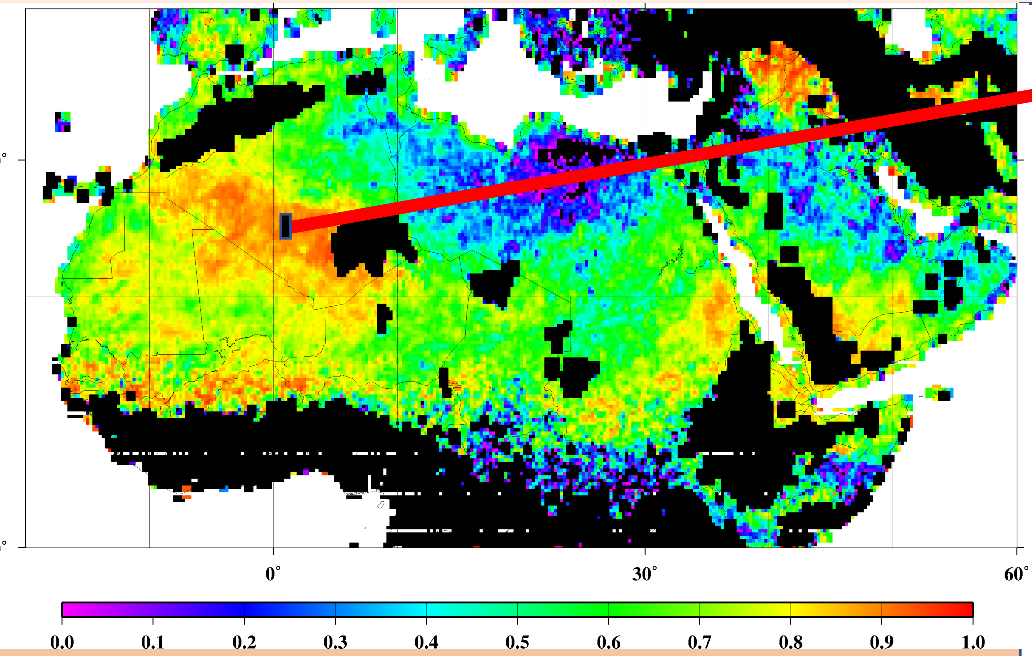

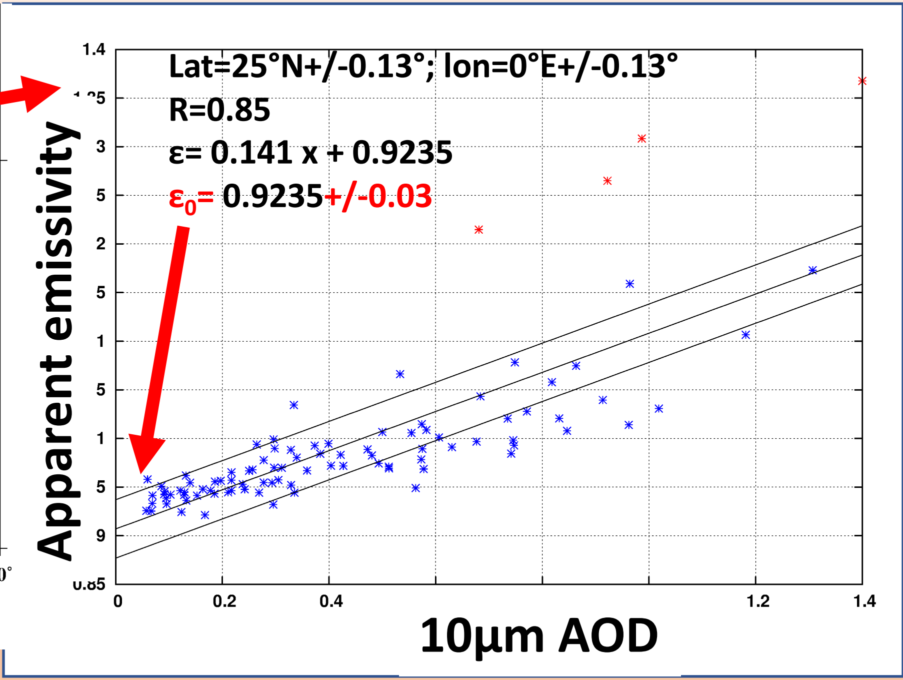

⇒ **AOD/emissivity correlation computed for each pixel of a 0.25° grid and for a selection of window channels**

⇒ **ε obtained by regression**

Validation : Seasonal variation at 8.3µm

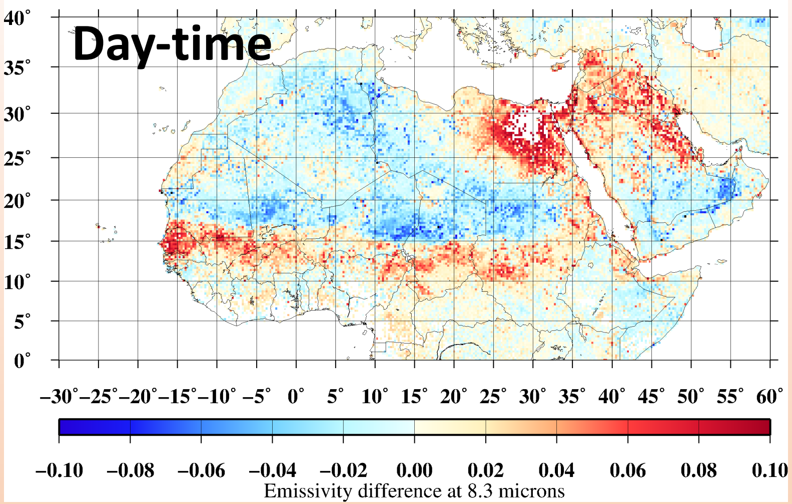

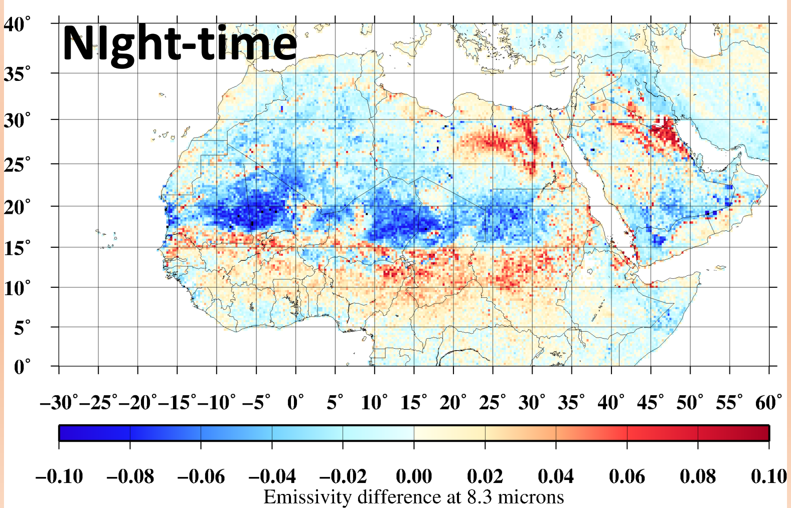

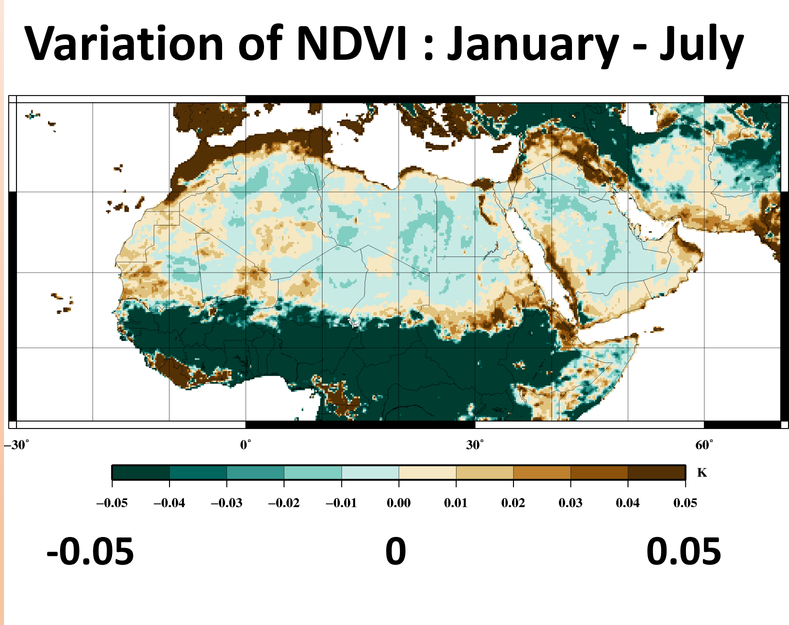

NIght-time

Validation : Seasonal variation at 4.63µm

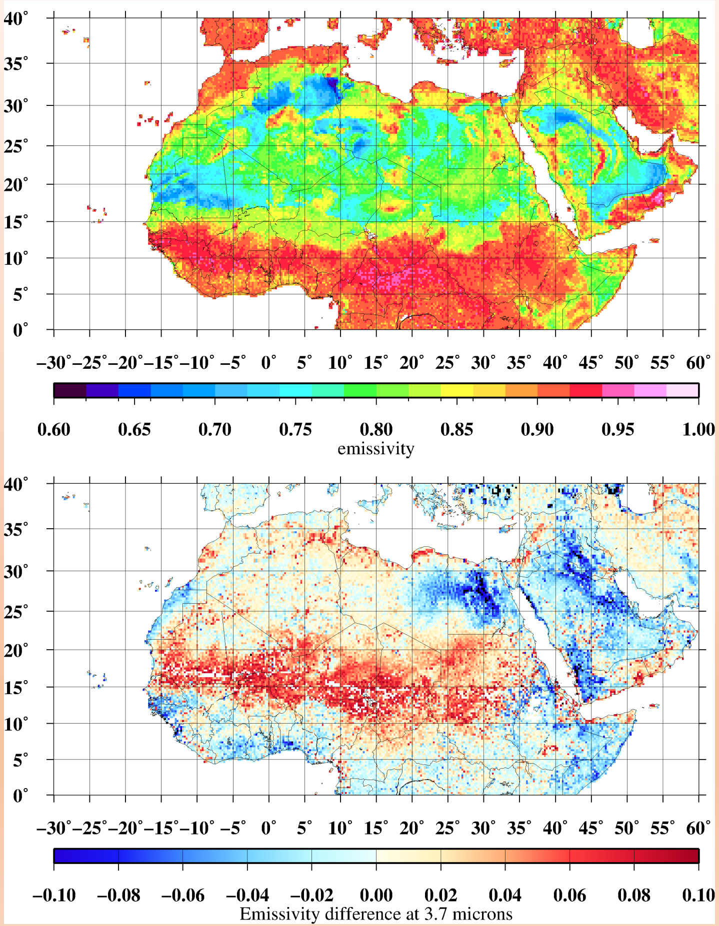

Variation of NDVI : January - July

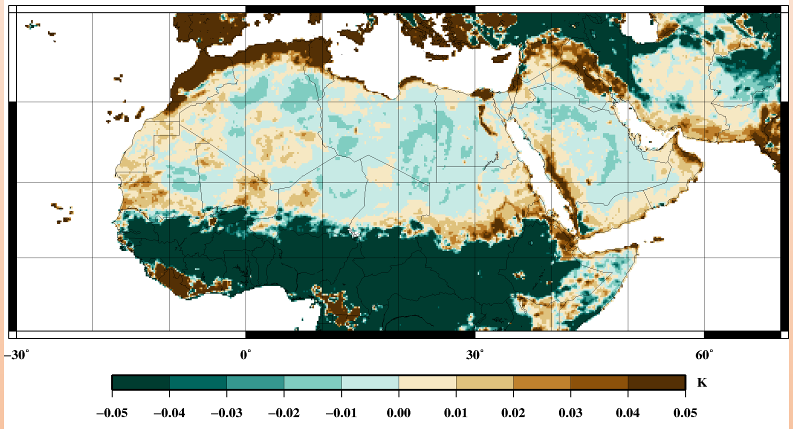

Validation :
use of 4A/OP + ARSA radiosounding database

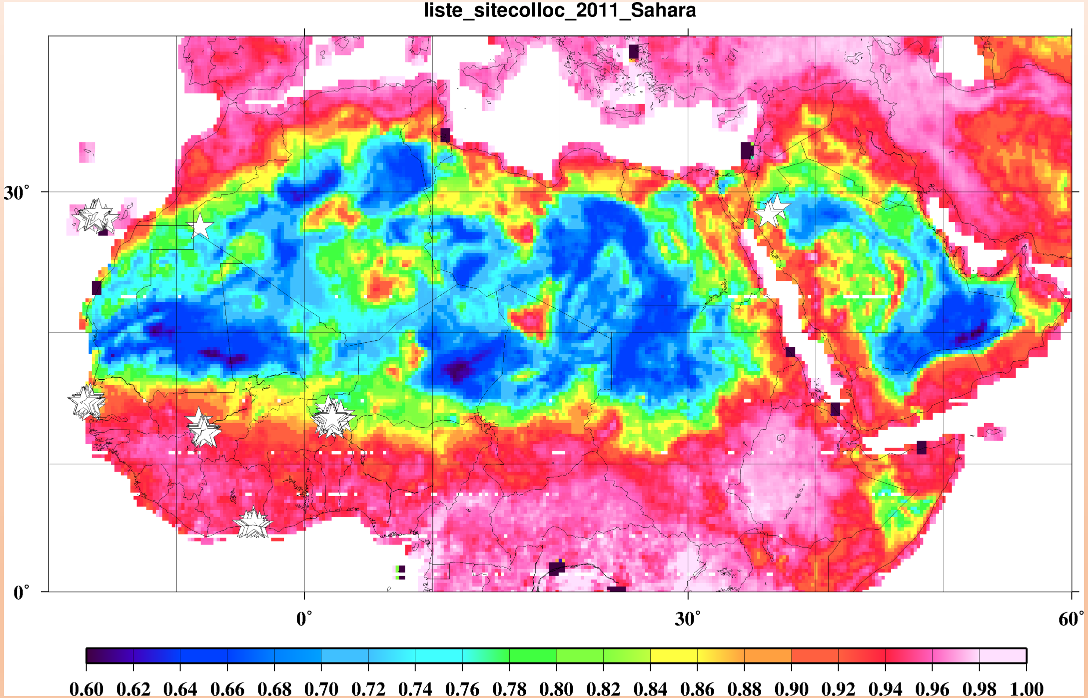

Collocation of IASI with the radio-sounding profile database ARSA
Year: 2011
Night-time conditions
~300 profiles
Surface temperature: MSM or L2-IASI

Validation : use of 4A/OP-SPARTE

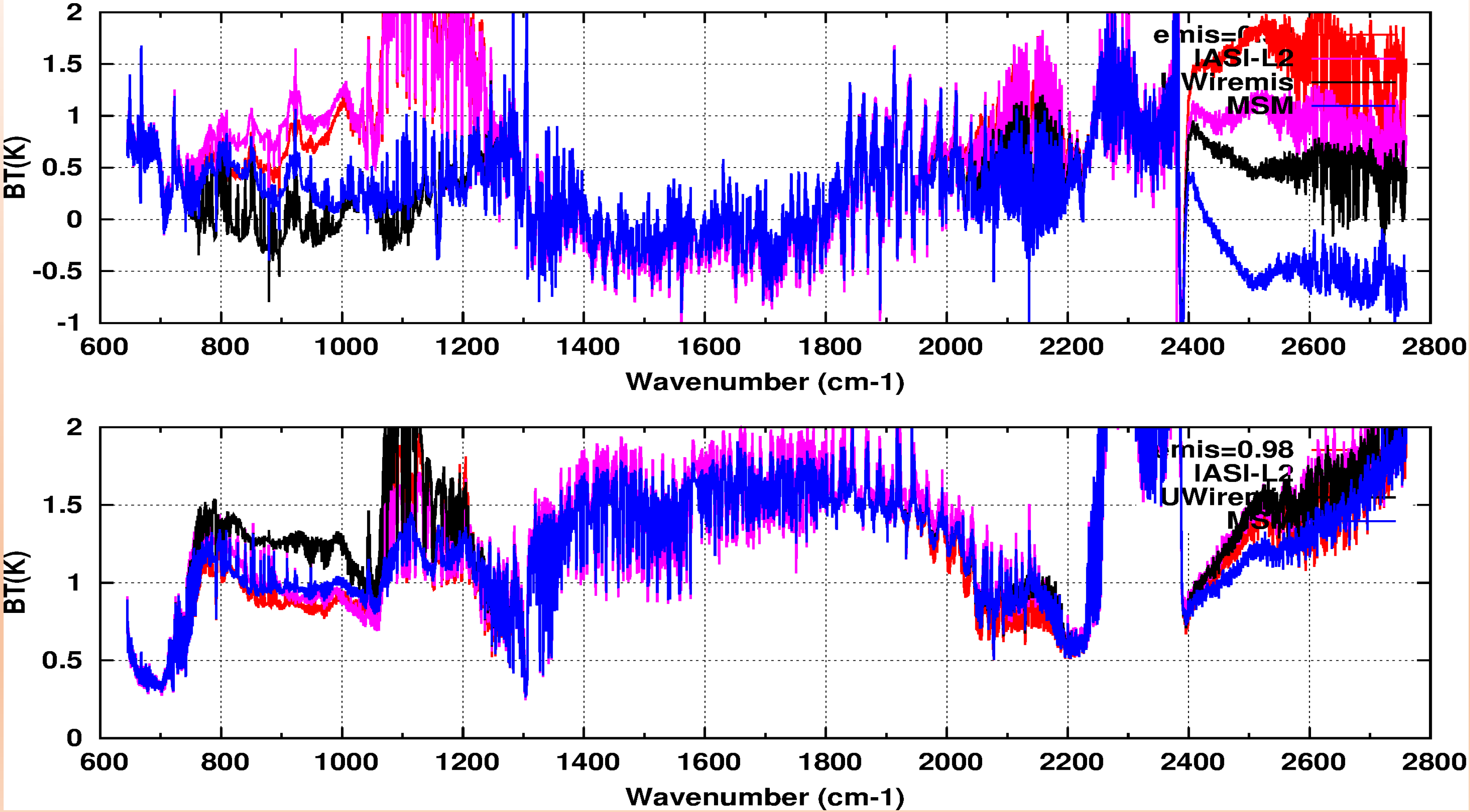

0.98

IASI-L2

UW HSR

MSM

Validation : use of 4A/OP-SPARTE

0.98
IASI-L2
UW HSR
MSM

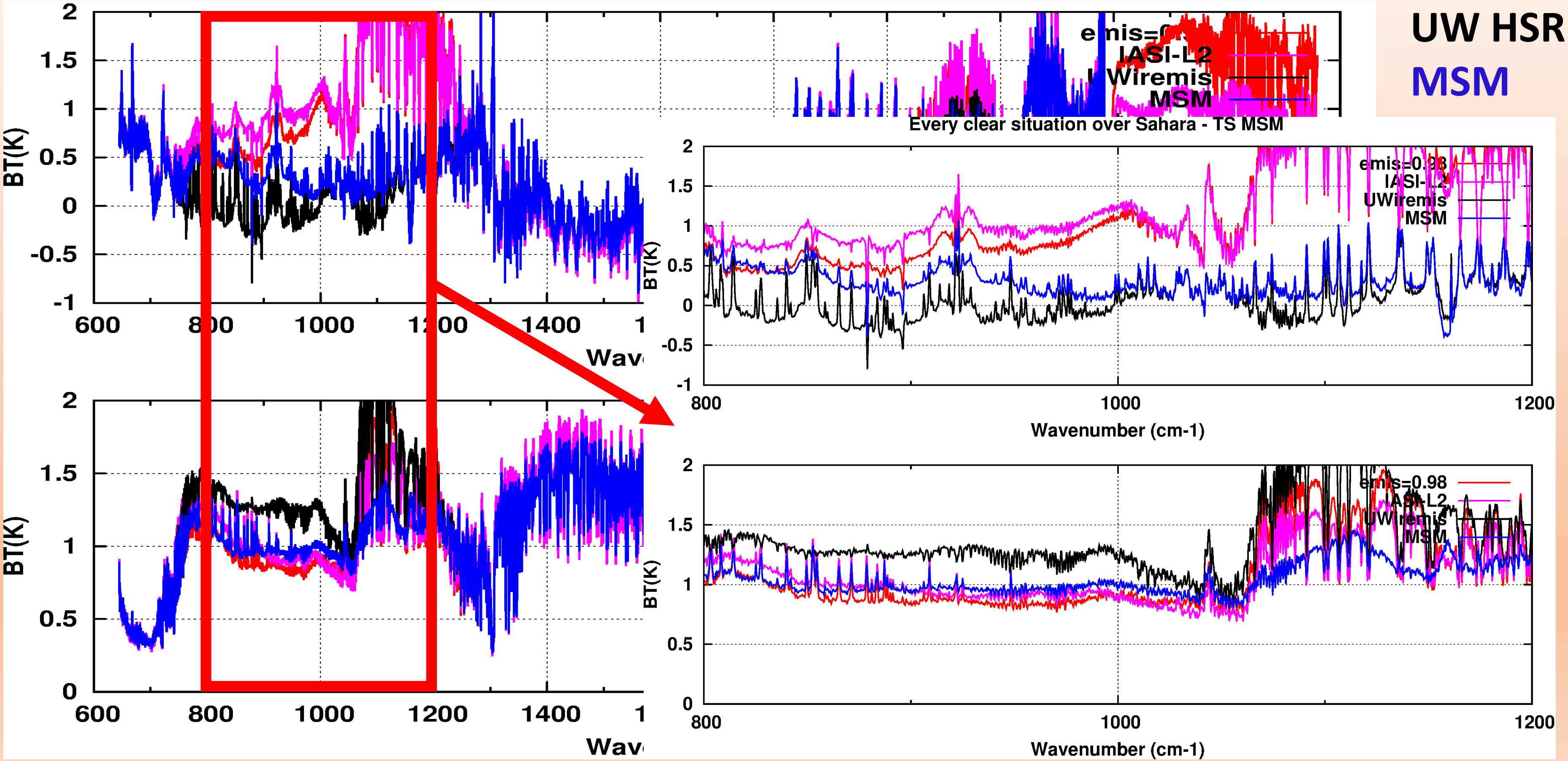

Validation : use of 4A/OP-SPARTE

0.98
IASI-L2
UW HSR
MSM

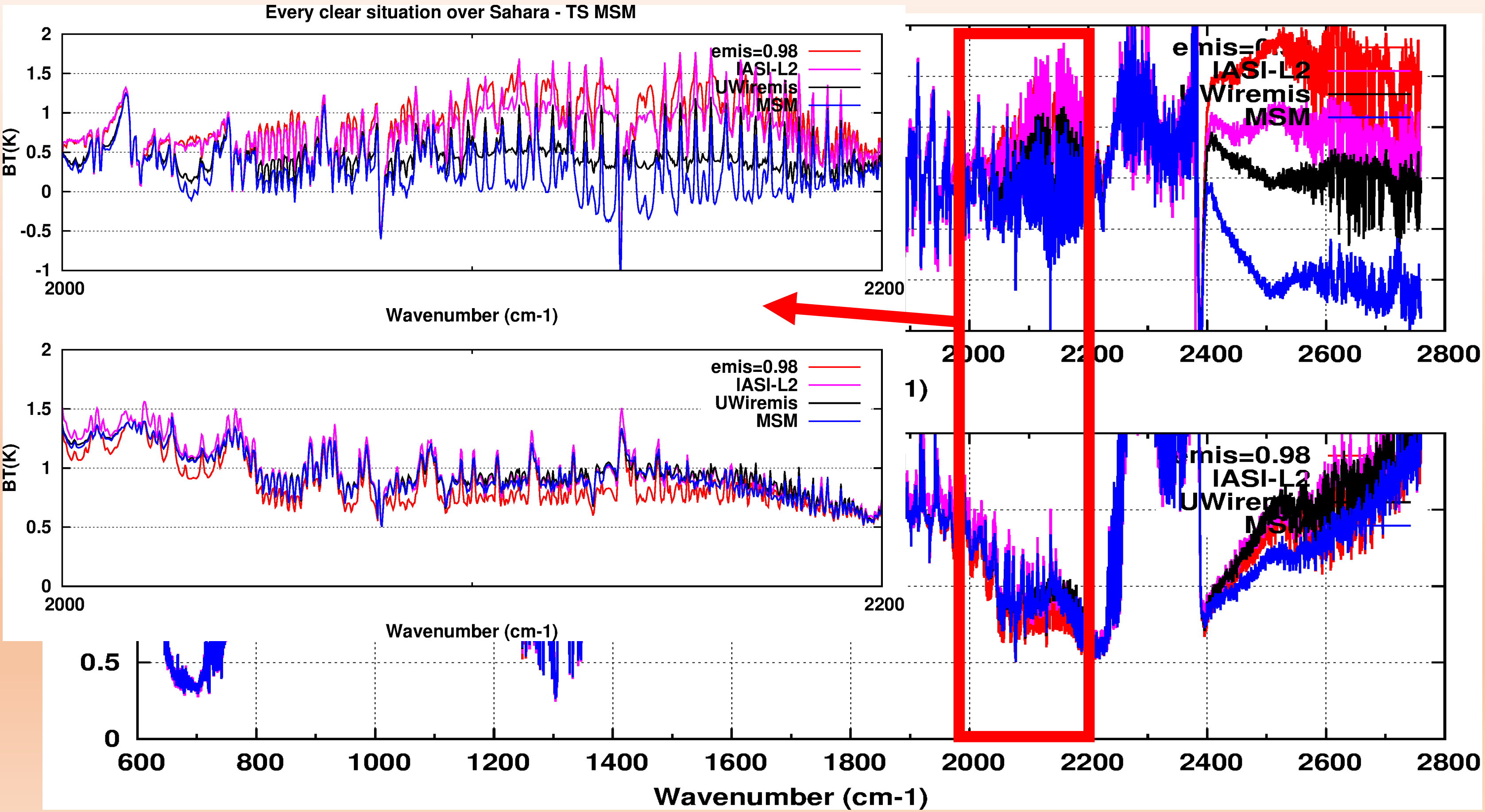

Validation : use of 4A/OP-SPARTE

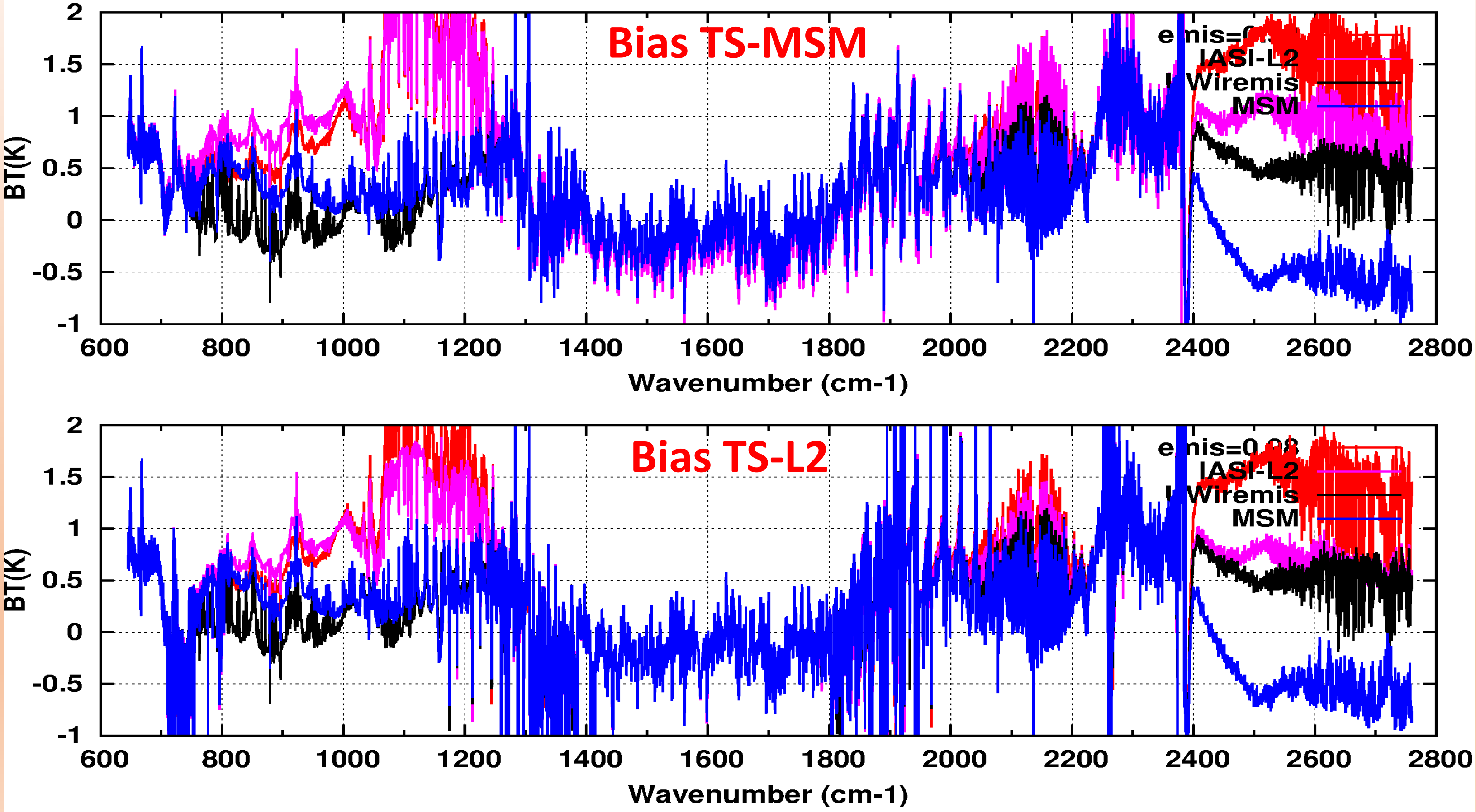

0.98

IASI-L2

UW HSR

MSM

Validation : use of 4A/OP-SPARTE

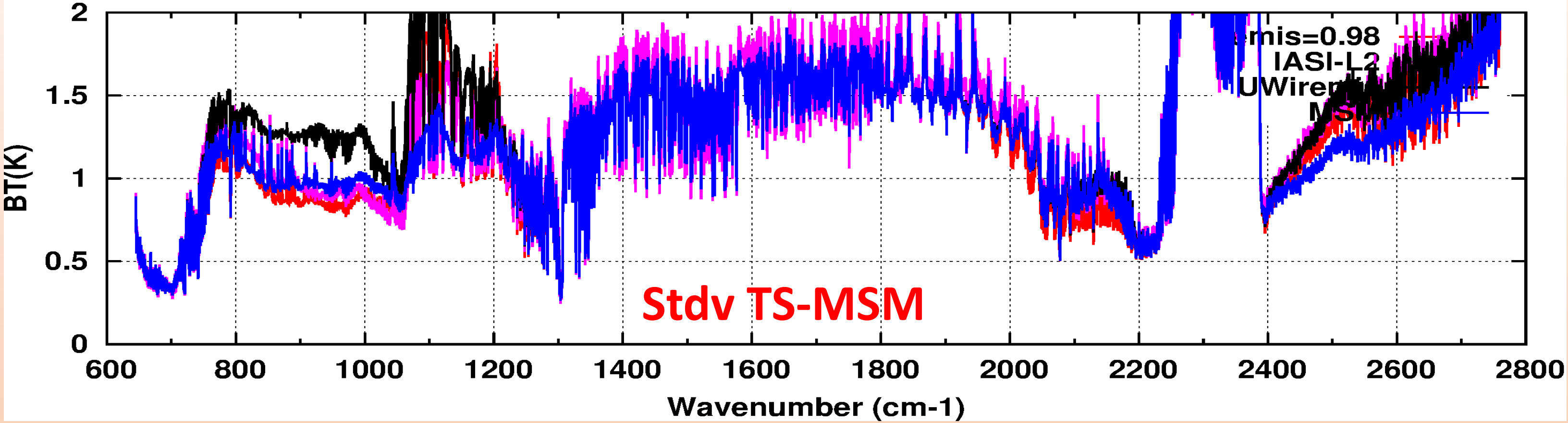

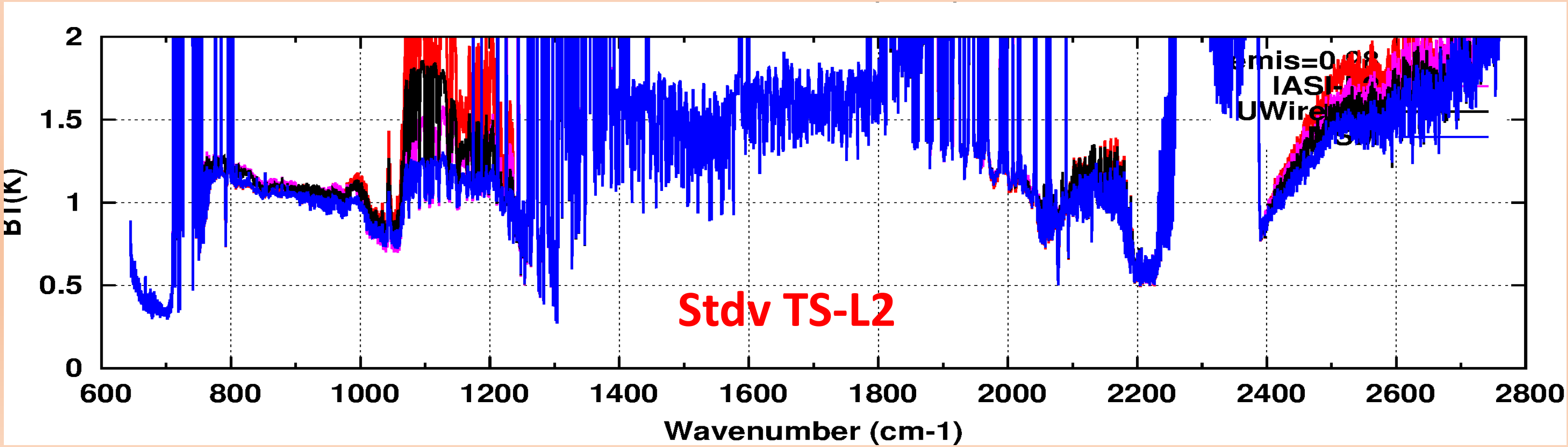

0.98
IASI-L2
UW HSR
MSM

Conclusion

- New IR surface emissivity database from IASI
- **Higher spatial resolution than previous (0.5° => 0.25°)**
- **High spectral resolution (0.05µm from 3.7 to 14µm)**
- **Clean from dust contamination**
- **Day and night separate**
- **Global**
- **Can be delivered in NRT (D-1) where AOD<0.15**
- Monthly => on-going

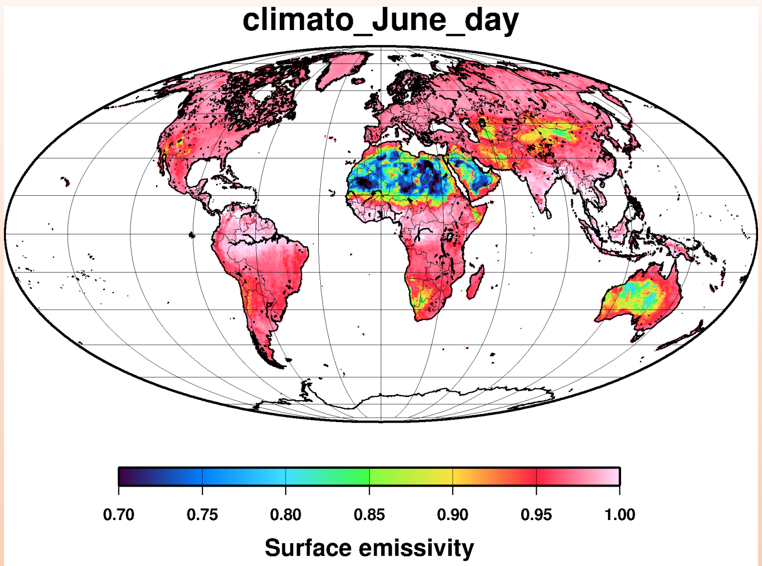

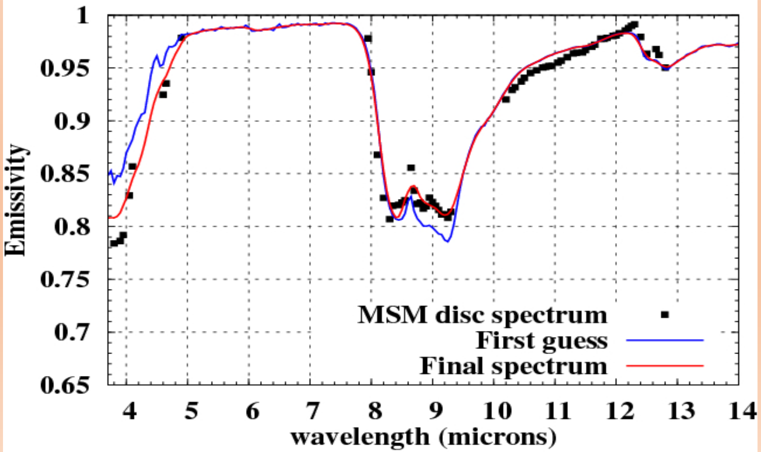

16 June 2013 –Day-time

Global and **daily** restitution in NRT (D-1) of :

- 10µm dust AOD
- Mean altitude
- Surface temperature
- Emissivity spectrum (if AOD<0.15)

Using **IASI/METOP-A** and **IASI-METOP-B**

IASIA+IASIB

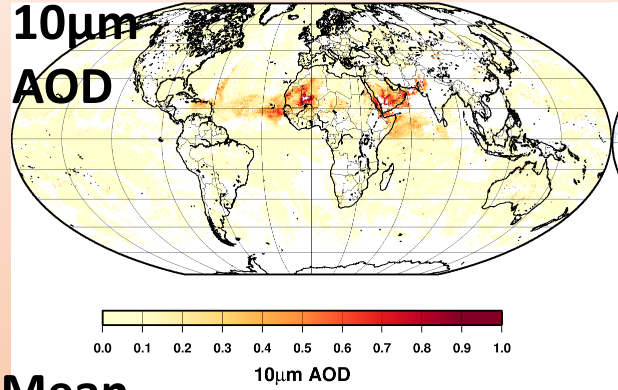

IASIA

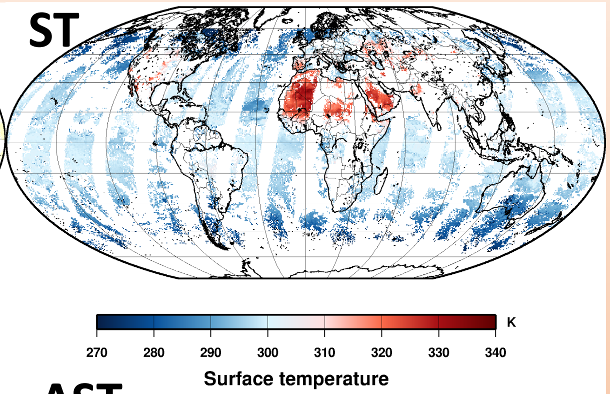

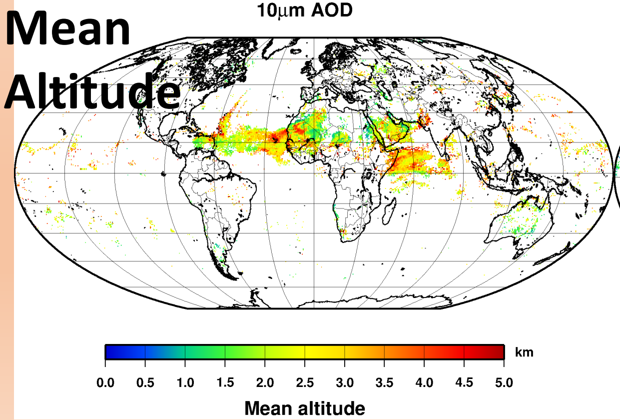

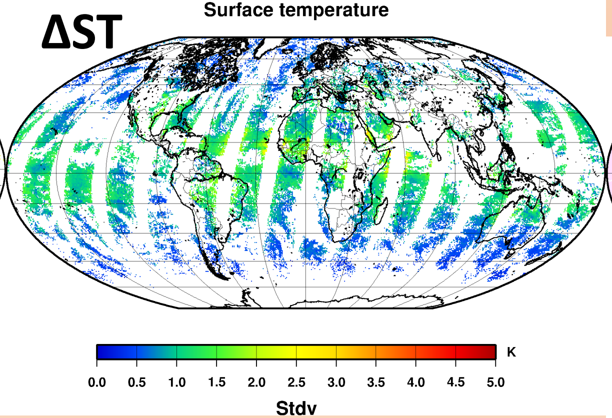

IASIA+IASIB

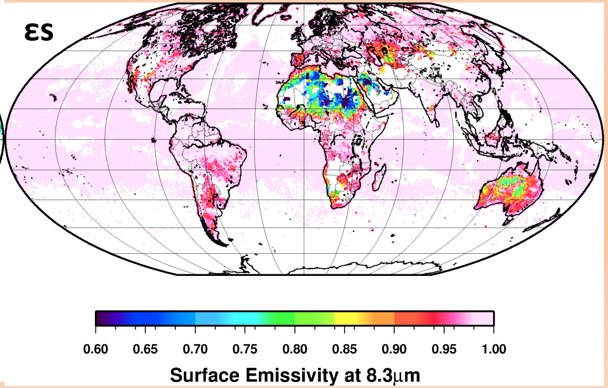

Conclusion

- Day and night variation analysis => on going

Night – Day at 8.3µm
January

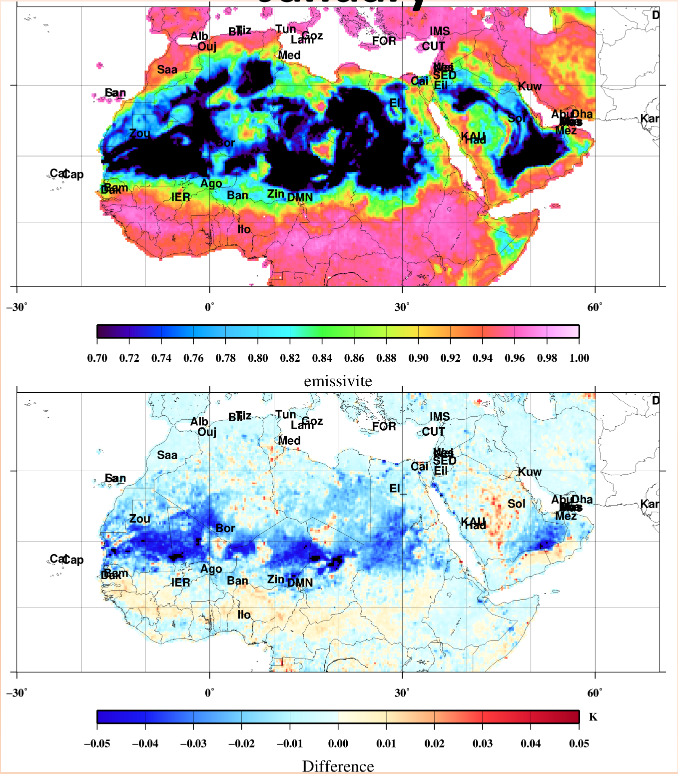

Night – Day at 8.3µm
July

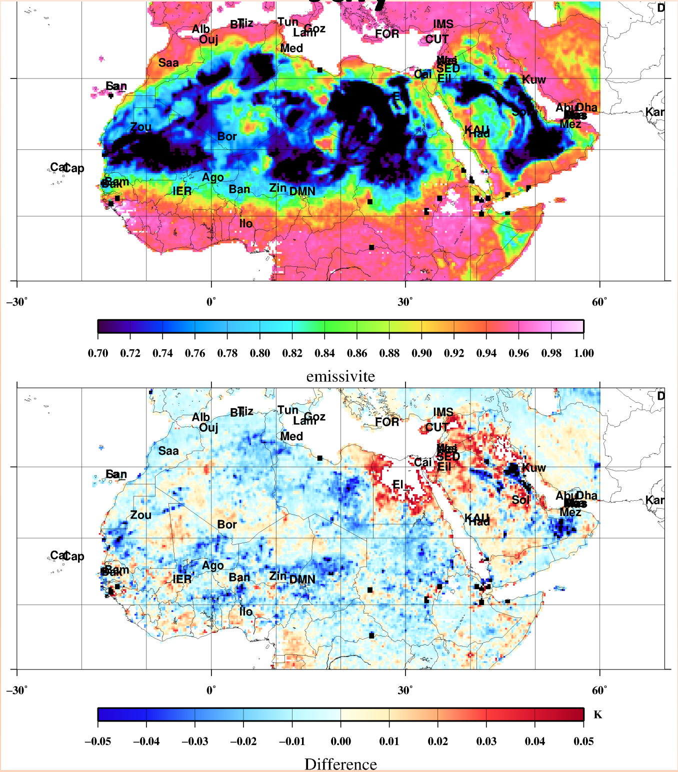

Infrared RTE (lambertian surface, clear sky, night)

$$I(\lambda,\theta) = \varepsilon_s(\lambda)\tau_s(\lambda,\theta)B(\lambda,T_s)$$ Surface Emission

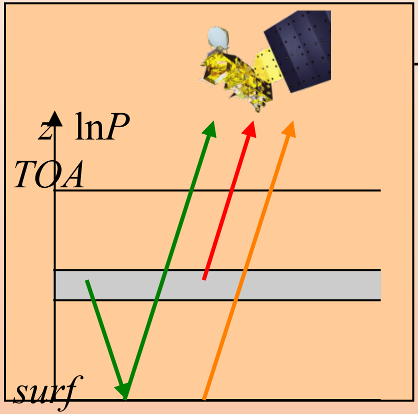

$$+\int_{\tau_s(\lambda,\theta)}^{1} B[\lambda,T]\,d\tau(\lambda,\theta)$$ Upwelling Atmosphere Emission

$$+(1-\varepsilon_s(\lambda))\tau_s(\lambda,\theta)\int_{\tau_s(\lambda,\theta)}^{1} B[\lambda,T]\,d\tau'(\lambda,\theta)$$ Reflected Downwelling Atmosphere Emission for a Lambertian surface

$$\tau'(\lambda,\theta)\tau(\lambda,\theta) = \tau_S(\lambda,\theta)$$

$$\varepsilon_s(\lambda) = \frac{I(\lambda,\theta) - \int_{\tau_s(\lambda,\theta)}^{1} B[\lambda,T]\partial\tau(\lambda,\theta) - \tau_s(\lambda,\theta)\int_{\tau_s(\lambda,\theta)}^{1} B[\lambda,T]\partial\tau'(\lambda,\theta)}{\tau_s(\lambda,\theta)\left\{B(\lambda,T_s) - \int_{\tau_s(\lambda,\theta)}^{1} B[\lambda,T]\partial\tau'(\lambda,\theta)\right\}}$$

Estimate the surface skin temperature

- **3 channels selected for their good transmittance (tau≥ 0.6) and a small variability of the emissivity (σ ~0.01):**

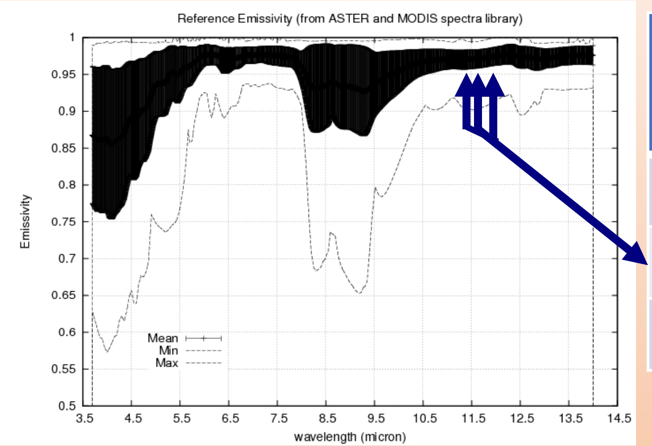

IASI channel	Mean ε	ε std dev
754 (12.µm)	0.975	0.012
867 (11.6µm)	0.971	0.013
921 (11.4µm)	0.970	0.013

- **ε~ 0.97 is no more an unknown for these channels and the skin temperature (T_s) remains the only unknown of the RTE.**

$$T_s = B^{-1}\left(\frac{I_{sat}(\lambda_0,\theta) - \int_{\tau_s(\lambda_0,\theta)}^{1} B[\lambda_0, T(\tau(\lambda_0,\theta))]\,d\tau - (1-\varepsilon_s(\lambda_0))\,\tau_s(\lambda_0,\theta) \int_{\tau_s(\lambda_0,\theta)}^{1} B[\lambda_0, T(\tau'(\lambda_0,\theta))]\,d\tau'}{\varepsilon_s(\lambda_0)\,\tau_s(\lambda_0,\theta)} \right)$$

- **Final surface temperature obtained by averaging the results from the 3 channels.**

Determination of the continuous emissivity spectrum

→ ε calculated for **101 "hinge points"**

→→→ **Discontinuous spectrum with a demonstrated accuracy accuracy better than 1.5% at 12 µm and ~4.5% at 4 µm.**

MSM emissivity database:

- 165 high spectral resolution emissivity laboratory measurements of different samples of typical Earth surfaces are selected from MODIS/UCSB and ASTER/JPL emissivity libraries.
- They are linearly interpolated at 0.05 µm resolution between 3.7 and 14.0 µm.

Proximity recognition + shape fit procedure

Emissivity continuous spectrum at 0.05 µm resolution between 3.7 and 14.0 µm

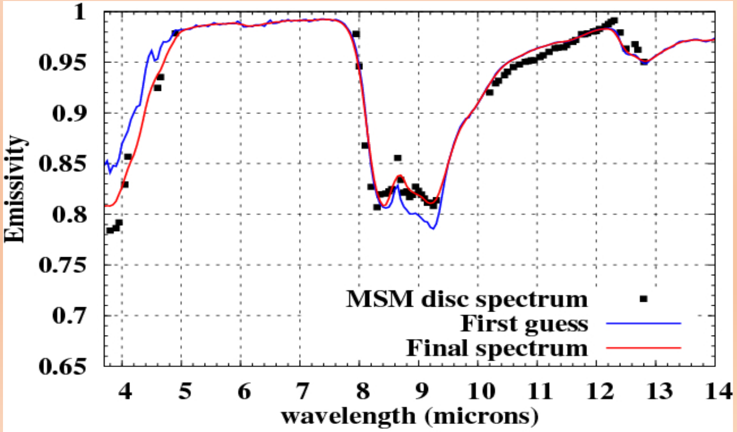

Perspective:
Introduction of BRDF in transfer modeling

Emissivity .vs. angle

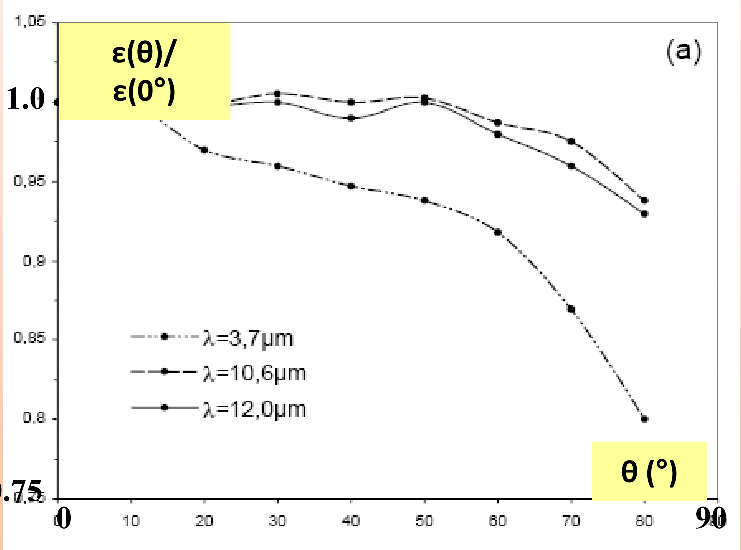

Labed J. and M.P. Stoll (1991), International Journal of Remote Sensing,

Angular variation impact on TIR emissivity:

- negligible impact in longwave (λ>4µm)

-Impact <5% for θ<40°

- impact even less given the spatial resolution of the observation

=> Introduction of BRDF may improve results for λ>4µm and/or θ>40°